Chapter 12
Hydrogen in Light-Metal Cage Assemblies: Towards a Nanofoam Storage

Fedor Y. Naumkin and David J. Wales

Abstract Isomeric alternatives to usual metal-hydrides as hydrogen-storage materials are considered. Presented are results of ab initio calculations for Be_n ($n \leq 18$) clusters with up to two endohedral H_2 molecules which undergo in-cage dissociation. The systems structures and stabilities are discussed, including energy barriers for hydrogen exit from the cage. The origin of the observed metastability, allowing for a lower-temperature release of H_2, is explored. Preservation of the cage integrity and hydrogen confinement is investigated when such core-shell units are merged into larger assemblies structurally resembling fragments of hydrogen-filled metal nanofoams, possible isomeric forms of metal-hydride solid. Different "nanofoam" isomers are composed of pairs or single H atoms suspended electrostatically inside the metal cage units ("nanobubbles"). Interesting features include simultaneous exit of two H atoms, etc. Structural extrapolations suggest potential hydrogen storage capacity up to ~10 weight-%.

12.1 Introduction

Reliable storage of hydrogen with an easy release on demand is a bottleneck problem of hydrogen-based energy solutions. Solid metal hydrides (e.g. MgH_2) offer high capacity but are so far problematic due to strong metal-H bonds needing high temperature (>300 °C for MgH_2) for releasing H_2 [1].

Corresponding clusters face similar problem, while being smaller and less rigid, both factors reducing the hydrogen-desorption temperature—see, e.g., recent advances for MgH_2-related species [2, 3]. Another class of such systems is represented by mixed/doped metal clusters M_nA_k (M = Be, B, Al; A = Li, Na, Mg, B, P, etc.), both physi- and chemisorbing hydrogen [4–7]. Here the hydrogen binding energies can be close to estimated ideal ~0.5 eV [1], larger or smaller up to negative values (corresponding to metastable systems, e.g. for CAl_{12} or $SiAl_{12}$ substrates [6, 7]), usually with ad-/desorption barrier of ~1 eV.

F.Y. Naumkin (✉)
Faculty of Science, UOIT, Oshawa, ON L1H 7K4, Canada
e-mail: fedor.naumkin@uoit.ca

M. Hotokka et al. (eds.), *Advances in Quantum Methods and Applications in Chemistry, Physics, and Biology*, Progress in Theoretical Chemistry and Physics 27,
DOI 10.1007/978-3-319-01529-3_12,

In particular, H_2 encapsulated in small Mg_n cluster cages can form weakly bound or even metastable species, although with a low storage capacity (∼1 weight-%) [8]. In order to try to improve the situation, the present work has two aims: (1) investigate similar systems of a lighter metal, Be; (2) evaluate feasibility of merging them into assemblies as a step to material.

Previous relevant work includes modeling adsorption of atomic H on solid Be (see [9] and references therein). The desorption temperature for molecular hydrogen has been predicted as ∼450 °C, with the desorption energy of ∼1 eV, which is even higher than for bulk MgH_2. Another family of systems studied have been BeH_2 aggregates and "polymers" [10], for which species, however, the hydrogen desorption temperature or energy has not been specified. The present work employs the earlier results indicating cage isomers of small Be_n clusters as most stable [11].

12.2 Computational Methods and Tools

Calculations have been carried out at the MP2/aug-cc-pvtz level, followed by the standard counterpoise BSSE correction [12]. This level of theory is employed as implemented in the NWChem ab initio package [13], and is preferred due to capability to deal reliably with anticipated non-covalent interactions and strong charge-transfer in the systems studied.

The system geometries have been fully optimized for all atomic coordinates, with no constraints (for the C_1 symmetry). Vibrational frequencies have been calculated to verify local minima of energy. The Be_n cages have been preoptimized, then hydrogen molecules have been put inside with different orientations, and the system then reoptimized. The potential energy barriers (e.g. for hydrogen exit from the cages) were estimated by pulling H in proper direction (e.g. through a gap between Be atoms): an appropriate Be–H distance was fixed at a series of values and all the other coordinates were reoptimized for each displacement.

Higher-spin states have been checked to confirm the ground state multiplicity. Natural charges on atoms have been calculated using the natural bonding orbital formalism [14].

12.3 Results and Discussion

12.3.1 H_2@Be_n

It is found that H_2 molecule can be trapped inside small Be_n clusters starting from $n = 8$ [15]. In particular, this and $n = 10$ cages generally preserve their shapes enveloping the dihydrogen oriented along their symmetry axis. This is different from the analogous case of Mg_8 cage which changes its shape [8]. Inside the Be_9 cage, however, the inserted molecule is trapped perpendicular to the original symmetry

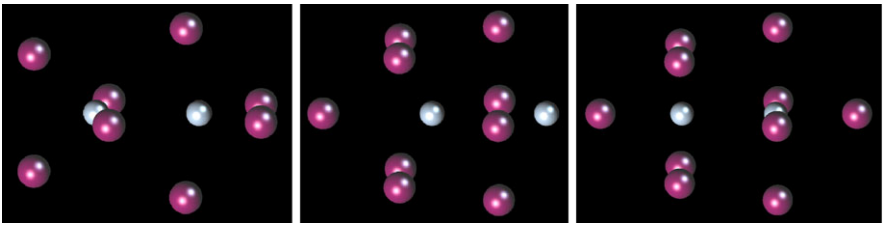

Fig. 12.1 Optimized geometries of $H_2@Be_8$, $H_2@Be_9$, $H_2@Be_{10}$

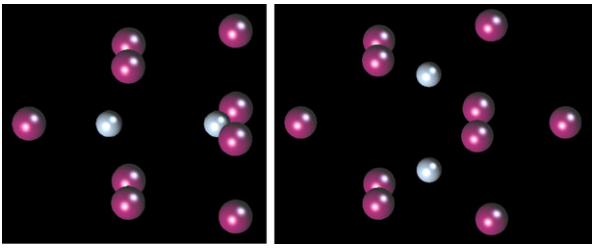

Fig. 12.2 Optimized geometries of higher-energy isomers of $H_2@Be_9$ and $H_2@Be_{10}$

axis of the cage which therefore transforms slightly, adopting a matching shape (capped square antiprism) now axially symmetric around the molecule. In all these cases, the H_2 molecule dissociates into H atoms suspended electrostatically (noncovalently) in the cage (Fig. 12.1).

For $n = 9$ one H atom protrudes from the cage, while adding another axial Be atom pushes it inside for $n = 10$. A higher-energy (by 1.7 eV relative to the isomer with the protruding H atom), "sunken" isomer of $H_2@Be_9$ has both H atoms inside the cage (Fig. 12.2), with a very low (∼0.04 eV) potential energy barrier separating this isomer from the more stable one. Another, "radial" isomer of $H_2@Be_{10}$ with the H_2 molecule perpendicular to the cage axis is 0.7 eV higher in energy (relative to the isomer with the axial orientation of H_2), with the potential energy barrier for turning the dihydrogen into axial orientation (in the lower-energy isomer) of only ∼0.06 eV.

The apparent reason for the H_2 molecule to dissociate is a considerable charge-transfer from the beryllium cage. According to calculations, each H atom is charged by −1.5e and −1.3e for $n = 8$ and 10, respectively. The high negative charge is apparently due to the number of Be atom neighbours donating the electron density. This charge is much larger than −0.15e for analogous $H_2@Mg_{10}$ [8], contrary to the opposite relation in the BeH and MgH diatoms as well as to the higher ionization energy of Be, but consistent with considerably shorter Be–H distances in $H_2@Be_n$. Accordingly, each Be atom is charged by +0.2e to +0.4e (Table 12.1).

For $n = 9$, the charge drops to −0.7e on the protruding H atom while remaining at −1.2e on the other one, the system asymmetry producing an axial dipole moment of 0.76 D. The two charges become about equal for the "sunken" isomer which, however, exhibits a fourfold dipole value of 3.1 D. The "radial" isomer of $H_2@Be_{10}$ is also slightly polar (0.35 D) due to the introduced slight asymmetry.

Table 12.1 Equilibrium parameters (in eV and Å) and atomic charges (in e) of $H_2@Be_n$

System	D_e^{total}/D_e[a]	R_e(H–H)	R_e(Be–H)	R_e(Be–Be)	q(H)	q(Be)
$H_2@Be_8$	11.41/−1.47	1.71	1.42	1.97–2.38	−1.56	0.36, 0.42
$H_2@Be_9$	17.30/1.44	1.96	1.68–1.87[b]	2.06–2.25	−1.19, −0.70[c]	0.17–0.32[d]
$H_2@Be_{10}$	18.98/−1.72	1.70	1.48–1.57[b]	2.13–2.22	−1.33	0.23, 0.41[d]

[a]For $H_2@Be_n \rightarrow H_2 + n$ Be / $\rightarrow H_2 + Be_n$

[b]To axial Be

[c]Protruding atom

[d]Axial atom

The Coulomb explosion of H_2 upon the shell-to-core charge-transfer is confined by the Be_n cage, which is the reason of the metastability of $H_2@Be_n$ for $n = 8$ and 10. These systems are, respectively, 1.5 and 1.7 eV higher in energy relative to the isolated relaxed molecule and cage. The $n = 9$ system, however, allows one H atom to stick outside, and, as a result, exhibits stability of 1.4 eV to such a dissociation. The "sunken" isomer of $H_2@Be_9$ is thus nearly iso-energetic with the dissociation products, such a stabilization relative to $n = 8$ and 10 being consistent with the "magic" number (20) of valence electrons in $H_2@Be_9$.

Calculations predict a low barrier of ∼0.06 eV for H atom to escape from the Be_8 cage which then opens up and lets both hydrogen atoms to surface. The resulting system is only marginally lower in energy (by 0.2 eV) than the original one, hence still metastable. For $n = 9$, the further axial withdrawal of the protruding H atom shows a similar barrier (∼0.08 eV), with the other H atom escaping to the surface as well. The Be_9 cage recovers its shape and the system further stabilizes by 1.3 eV relative to the original one. For $n = 10$, however, the barrier experienced by H atom on its way to the cage surface reaches 0.6 eV, the resulting system having almost the same (marginally higher) energy as original $H_2@Be_{10}$. However, the cage distorts and, as a result, the other hydrogen atom can leave the cage with almost no barrier. This lowers the system energy by 2.2 eV, thereby making it stable by about 1 eV to dissociation into Be_{10} and H_2.

The relative stabilities of $H_2@Be_n$ to dissociation into $H_2 + Be_n$ are reflected in their total dissociation energies D_e^{total} (into $H_2 + n$ Be) as compared to those for respective Be_n. Metastable $H_2@Be_8$ and $H_2@Be_{10}$ have D_e^{total} decreased relative to the original cages by about 0.2 eV per Be atom, while $H_2@Be_9$ is stabilized by a similar amount relative to relaxed Be_9. The overall trend of D_e^{total} increasing with n (in the range of 1.4–1.9 eV per Be atom) is, however, preserved (see Table 12.1).

12.3.2 $(H_2)_2@Be_n$

Both $H_2@Be_8$ and $H_2@Be_{10}$ are employed as units in cluster assemblies [16]. Merging two $n = 8$ systems axially via two shared atoms produces $(H_2)_2@Be_{14}$

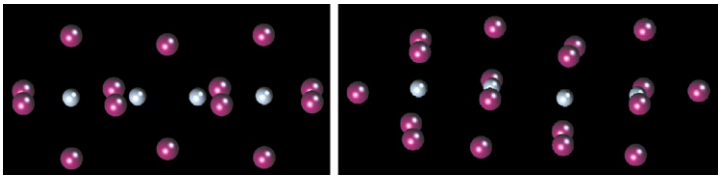

Fig. 12.3 Optimized geometries of $(H_2)_2@Be_{14}$ and $(H_2)_2@Be_{18}$

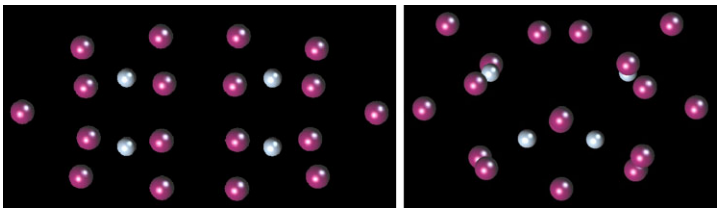

Fig. 12.4 Optimized geometries of "radial" $(H_2)_2@Be_{18}$ and $(H_2)_2@Be_{17}$

with slightly zig-zagging chain of four H atoms inside the Be_{14} cage (Fig. 12.3). The system is triply more metastable, being 4.3 eV above the relaxed cage plus two hydrogen molecules, as compared to $H_2@Be_8$, while the barrier for escape of H remains about same.

A similar situation is found when axially merging two $n = 10$ units while removing two Be atoms. In fact, the resulting system resembles two $H_2@Be_9$ units joined by their open ends, with protruding H atoms being pushed back inside (Fig. 12.3). The system is twice as high in energy (by 3.4 eV) relative to relaxed $Be_{18} + 2H_2$ as $H_2@Be_{10}$ relative to $Be_{10} + H_2$, the difference from the $(H_2)_2@Be_{14}$ versus $H_2@Be_8$ case being due to longer distances between the hydrogen anions (Table 12.2).

The higher-energy isomers of $H_2@Be_{10}$ can also be merged in a similar way, in which case, however, the resulting $(H_2)_2@Be_{18}$ isomer is only 2.4 eV above $Be_{18} + 2H_2$, i.e. significantly lower in energy than the previous isomer. The apparent reason of this is a larger distance between the hydrogen diatoms oriented perpendicularly, even though each "radial" $H_2@Be_{10}$ unit is higher in energy.

Finally, two $H_2@Be_{10}$ units have been merged via a shared triatomic Be_3 face at their ends, with the units twisting relative to one another to adopt a staggered arrangement of atoms at the other ends. The resulting $(H_2)_2@Be_{17}$ system is composed of a C-shaped chain of four H atoms inside a bent Be_{17} cage (Fig. 12.4). An interesting feature of this species is its almost identical metastability (about 1.7 eV higher in energy than relaxed $Be_{17} + 2H_2$) as compared to that of $H_2@Be_{10}$.

In all above systems, the charges on the H atoms only slightly reduce (by 0.2e for $(H_2)_2@Be_{14}$ and 0.1e for the $H_2@Be_{10}$-based species) relative to those in the respective units (Table 12.2). This, together with shorter distances between the hydrogen anions in $(H_2)_2@Be_{17}$ as compared to "radial" $(H_2)_2@Be_{18}$, could not explain such a stabilization of the former. One possible interpretation could be based

Table 12.2 Equilibrium parameters (in eV and Å) and atomic charges (in e) of $(H_2)_2@Be_n$

System	D_e^{total}/n; D_e[a]	R_e(H–H)	R_e(Be–H)	R_e(Be–Be)	q(H)	q(Be)
$(H_2)_2@Be_{14}$	1.73; −4.25	1.46[b], 1.63	1.39–1.72	1.95–2.58	−1.27, −1.30[c]	0.15–0.46[d]
$(H_2)_2@Be_{18}$	2.08; −3.45	1.80, 1.82[b]	1.48–1.67	2.05–2.48	−1.15[c], −1.23	0.04–0.38[d]
"Radial"	2.14; −2.36	1.56	1.37–1.62	2.09–2.46	−1.22	0.05–0.43[d]
$(H_2)_2@Be_{17}$	2.14; −1.71	1.74–1.78[b]	1.45–1.78	2.05–2.35	−1.16[c], −1.20	0.09–0.45[e]

[a] $\rightarrow 2H_2 + nBe$; $\rightarrow 2H_2 + Be_n$

[b] Between inner H atoms

[c] Inner H atoms

[d] Outermost Be atoms

[e] Innermost shared Be atom

on the specific structure with Be atoms located between H atoms and resulting in a charge distribution "negative-positive-negative" creating a significant quadrupole moment of such a layered centre polarizing the outer beryllium atoms.

In addition, the $(H_2)_2@Be_{17}$ system exhibits a significant stability to the hydrogen escape from the cage, with the potential energy barrier of 0.3 eV. This is a half of the barrier for the $H_2@Be_{10}$ unit, the reduction likely being due to increased repulsion between the larger number of closely-spaced hydrogen anions.

Further 1D structural extension of the above $(H_2)_2@Be_{14}$ and $(H_2)_2@Be_{18}$ systems into a beryllium "nanotube" with a hydrogen "wire" inside by adding more units would lead to the hydrogen storage capacity up to 3.6 and 2.7 weight-% (one H per three and four Be), respectively. This value could be increased via merging the units by their sides as well, i.e. for 2D and 3D extensions. In particular, when the $(H_2)_2@Be_{10}$ units are merged by a shared Be_3 face at their ends, as in the above $(H_2)_2@Be_{17}$ system, the storage capacity is evaluated to have an upper limit of about 8 weight-%.

12.3.3 $H_k@Be_n$

Since H_2 dissociates in Be_n, encapsulation of separate H atoms in such cages has been considered as well [17]. The Be_6 cluster is found to be the smallest one able to accommodate an H atom inside. The centrally positioned hydrogen atomic core transforms the beryllium shell from a bipyramid into a perfect octahedron (Fig. 12.5). Unlike the metastable $H_2@Be_{10}$ counterpart, the system is stable to dissociation into relaxed $Be_6 + H$ by appreciable 1.7 eV. The isomers with H attached to Be_6 outside are more stable (bound by 3 eV), both Be_2-edge and Be_3-face sites being nearly degenerate (within 0.1 eV). The barrier for the hydrogen exit from the cage is found to be 0.5 eV.

In endohedral $H@Be_6$, the H atom is charged by −0.95e, which is only slightly more negative than −0.8e for the other, HBe_6 isomers. The charge on H is smaller

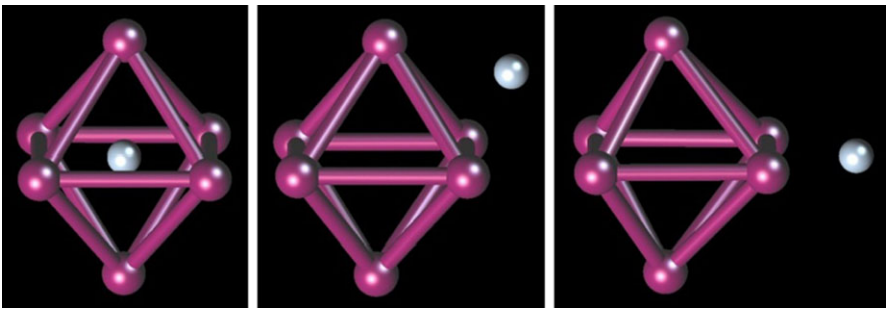

Fig. 12.5 Optimized geometries of endohedral H@Be_6 and two HBe_6 isomers

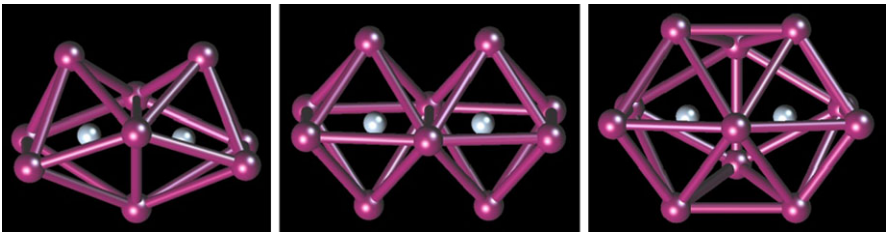

Fig. 12.6 Optimized geometries of (2H)@Be_9, (2H)@Be_{10}, and (2H)@Be_{11}

than in H_2@Be_{10}, even though in the latter case each hydrogen atom has less neighbouring electron-density donors.

The stability of the H@Be_6 species suggests a possibility of building larger assemblies from such blocks. Merging two H@Be_6 units via a shared Be_3 face produces a (2H)@Be_9 species with the units distorted but generally preserved (Fig. 12.6). The repulsion of two hydrogen anions makes the system metastable, 1.2 eV above relaxed $Be_9 + H_2$, hence a higher-energy isomer relative to the above H_2@Be_9. When empty, the relaxed beryllium cage generally preserves its shape of two face-merged Be_6 units, as a higher-energy isomer of Be_9. Due to strain in the system, the barrier for H exit from the cage reduces to 0.2 eV. The two hydrogen centres close to one another in (2H)@Be_9 carry significantly increased negative charges as compared to H@Be_6, $-1.4e$ on each, in spite of the smaller number of Be atoms per H. The system has a small dipole moment of 0.2 D, close to that for the (H_2)@Be_{17} counterpart.

When two H@Be_6 units are merged via a shared Be_2 edge, a (2H)@Be_{10} system is produced (Fig. 12.6), with the shared edge stretched. The H anions are slightly further apart as compared to (2H)@Be_9 (see Table 12.3), which stabilizes the system which is now 0.8 eV above relaxed $Be_{10} + H_2$. This value is a half that for (H_2)@Be_{10}, but is relative to the relaxed empty beryllium cage preserving its shape of two Be_6 edge-sharing units, which is a higher-energy isomer of Be_{10}. As a result, (2H)@Be_{10} remains 1.9 eV higher in energy as compared to (H_2)@Be_{10}. The po-

Table 12.3 Equilibrium parameters (in eV and Å) and atomic charges (in e) of (kH)@Be_n

System	D_e^{total}[a]/n; D_e[b]	R_e(H–H)	R_e(Be–H)	R_e(Be–Be)	q(H)	q(Be)
H@Be_6	1.56; 1.72		1.51	2.13	−0.95	+0.08–0.31
(2H)@Be_9	1.62; −1.19	1.68	1.50–1.72	2.14–2.43	−1.38	+0.15–0.42
(2H)@Be_{10}	1.71; −0.77	1.95	1.51–1.58	1.96–2.48	−1.26	−0.08–+0.40
(2H)@Be_{11}	1.94; −1.52	1.71	1.51–2.01	2.01–2.24	−1.21	+0.11–0.35
(3H)@Be_{11}	1.99; 0.41	1.67	1.52–1.69	1.99–2.32	−1.36	+0.16–0.46

[a] (kH)@$Be_n \rightarrow n\mathrm{Be} + \mathrm{H}/\mathrm{H}_2/(\mathrm{H}+\mathrm{H}_2)$ for $k = 1/2/3$

[b] (kH)@$Be_n \rightarrow \mathrm{Be}_n + \mathrm{H}/\mathrm{H}_2/(\mathrm{H}+\mathrm{H}_2)$ for $k = 1/2/3$

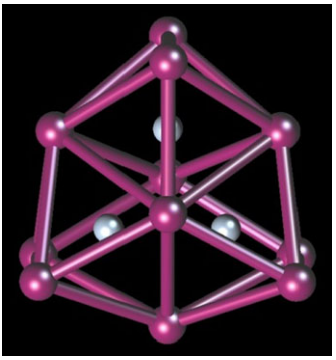

Fig. 12.7 Optimized geometry of (3H)@Be_{11}

tential energy barrier between the two isomers is 0.15 eV, and this isomerization occurs along the pathway followed by H atom exiting the cage.

An attempt to separate the H anions even further by merging two H@Be_6 units via a shared atom results in a collapse of the units into a Be_{11} cage encapsulating both H atoms (Fig. 12.6). The (2H)@Be_{11} system is metastable, being higher in energy than relaxed $Be_{11} + H_2$ by 1.5 eV which is the largest value among those for (2H)@Be_n, $n = 9$–11. The Be–Be interactions holding the cage together thus overcome the repulsion of the hydrogen anions. The charges on the H atoms slightly decrease with increasing n (Table 12.3), to −1.2e for $n = 11$, opposite to the number of the donating Be atoms. The asymmetry of the cage leads to a small dipole moment of 0.34 D.

As a next step, a third H@Be_6 unit is merged to (2H)@Be_9 via two shared Be_3 faces, leading to a D_{3h}-symmetric (3H)@Be_{11} assembly with three H atoms forming an equilateral triangle (Fig. 12.7). The beryllium frame keeps its shape when empty, the (3H)@Be_{11} system being weakly stable by 0.4 eV to dissociation into relaxed $Be_{11} + H_2 + H$. Such a stabilization of (3H)@Be_{11} can be viewed as being due to combination of metastable (2H)@Be_9 and stable H@Be_6. An alternative channel is represented by dissociation into (2H)@$Be_{11} + H$, in which case the above $n = 11$ species with two H atoms is recovered. These products correspond to the dissociation energy of 0.6 eV. The barrier for H atom exit from the cage is back to 0.5 eV

(as for $H@Be_6$), apparently due to a lower strain in the beryllium cage. The charge on each of the H atoms is $-1.4e$, same as for $(2H)@Be_9$.

Similar to $(H_2)@Be_n$, the relative stabilities of the above $(kH)@Be_n$ systems to separation into the hydrogen and beryllium components translate into their total dissociation energies D_e^{total} (corresponding to Be_n dissociated into atoms). Inserting H into Be_6 and $H + H_2$ into $Be_{11}(D_{3h})$ stabilizes these clusters, significantly (by 0.3 eV per Be atom) for the former and slightly for the latter. While insertion of H_2 into Be_9, Be_{10} and Be_{11} destabilizes them by about 0.1 eV per Be atom. Overall, the D_e^{total} values increase with the system size, as for $(H_2)@Be_n$, from 1.6 to 2 eV per Be atom (Table 12.3).

12.4 Conclusions

Beryllium cluster cages form metastable (by a few eV) core-shell systems when endohedrally doped by molecular hydrogen dissociating due to a strong electron donation from, and confined in, the cage. When small $H_2@Be_n$ units are merged together, they can generally preserve shapes and integrity in the larger assemblies. In some cases, this can result in a further stabilization of the system, as for $(H_2)_2@Be_{17}$. Another feature is a possible higher stability of the assemblies composed of higher-energy isomers of the units, as for $(H_2)_2@Be_{18}$. Energy barriers to extraction of H_2 can be low ($\sim$0.1 eV for $n = 8, 9, 14$) to appreciable ($\sim$0.6 eV for $n = 10$), suggesting low-temperature conditions for stabilization. Extraction of both H atoms at once is more likely.

The metastability may offer two benefits: (1) easier release of hydrogen, (2) direct storage of extra energy ($\sim$0.5–2 eV per H_2 molecule here). Hydrogen storage capacity can be increased in cluster assemblies/materials, e.g. nanofoams. This is confirmed for face-sharing $H_2@Be_{10}$ units, with extrapolated upper bound of $\sim$8 weight-%. Feasibility of such materials is supported experimentally by a recent progress reported for Mg [18].

Such an endohedral doping may also offer options for modification of mechanical and electronic characteristics (shape, dipole moment) of clusters. This suggests potential applications in nanomaterials and molecular electronics.

Be_6 is able to accommodate H atom inside and is significantly stable (by $\sim$2 eV) to its release. This stability can be reduced by design via merging such units into assemblies which are metastable to release of molecular H_2, with a desorption barrier of $\sim$0.5 eV (matching the suggested ideal binding energy [1]). Hydrogen storage capacity of such systems extrapolated to a nanofoam material, composed of face-sharing $H@Be_6$ units filling space, can reach $\sim$10 weight-%. This may exceed the value for the counterparts with encapsulated H_2 (e.g. inside Be_{10} units) due to higher symmetry and better packing.

Such cluster-assembled materials could be more straightforward to develop than macro-assemblies of clusters preserving multiple surface sites for external binding of H_2 molecules. Firm conclusions, however, would benefit from relevant experiments as well as modelling of molecular dynamics related to hydrogen entering and

exiting the cages, in particular for refilling the nanofoam. It is hoped that the present work will stimulate such studies in the near future.

Acknowledgements The authors thank the RSC and the NSERC of Canada for the financial support of this work via a travel grant to FN. The staff of the HPC facilities of the UOIT Faculty of Science and of the Sharcnet network of Ontario are acknowledged for their invaluable technical support. FN is grateful to the University of Cambridge Department of Chemistry for their hospitality during his sabbatical visit.

References

1. Graetz J (2009) Chem Soc Rev 38:73
2. Wagemans RWP et al (2005) J Am Chem Soc 127:16675
3. Harder S et al (2011) Angew Chem, Int Ed 50:4156
4. Srinivasu K et al (2012) RSC Adv 2:2914
5. Bandaru S et al (2012) Int J Quant Chem 112:695
6. Wang L et al (2009) J Comput Chem 30:2509
7. Henry DJ, Yarovsky I (2009) J Phys Chem A 113:2565
8. McNelles P, Naumkin FY (2009) Phys Chem Chem Phys 11:2858
9. Allouche A (2008) Phys Rev B 78:085429
10. Lingam CB et al (2011) Comput Theor Chem 963:371
11. Sun Y, Fournier R (2005) Comput Lett 1:1
12. Boys SF, Bernardi F (1970) Mol Phys 19:553
13. Valiev M et al (2010) NWChem, version 6.x. Comput Phys Commun 181:1477
14. Reed AE, Curtiss LA, Weinhold F (1988) Chem Rev 88:899
15. Naumkin FY, Wales DJ (2012) Int J Quant Chem 112:3068
16. Naumkin FY, Wales DJ (2011) J Phys Chem A 115:12105
17. Naumkin FY, Wales DJ (2012) Chem Phys Lett 545:44
18. Skorb EV et al (2010) Nanoscale 2:722